10Gbps Operation of a Metamorphic InGaP Buffered $In_{0.53}Ga_{0.47}As$ p-i-n Photodetector Grown on GaAs Substrate

Yu-Sheng Liao[1], Gong-Ru Lin[1*], Chi-Kuan Lin[1], Yi-Shiang Chu[1], Hao-Chung Kuo[1], Milton Feng[2]
[1]Department of Photonics & Institute of Electro-Optical Engineering,
National Chiao Tung University,
1001, Ta Hsueh Rd., Hsinchu, Taiwan 300, R. O. C.
[2] Department of Electrical and Computer Engineering, Microelectronic Laboratory
University of Illinois at Urbana-Champaign
Urbana, IL 61801, USA
[*]Corresponding author. Phone: 886-3-5712121 ext. 56376; Fax: 886-3-5716631; E-mail: grlin@faculty.nctu.edu.tw

ABSTRACT

A novel top-illuminated $In_{0.53}Ga_{0.47}As$ p-i-n photodiodes (MM-PINPD) grown on GaAs substrate by using a linearly graded metamorphic $In_xGa_{1-x}P$ (x graded from 0.49 to 1) buffer layer has been demonstrated on the SONET OC-192 receiving performance. With a cost-efficient TO-46 package, the MM-PINPD at data rate of 10 Gbit/s can be obtained at minimum optical power of -19.5 dBm. At wavelength of 1550nm, the dark current, optical responsivities, noise equivalent power, and operational bandwidth of the MM-PINPD with aperture diameter of 60 μm are 13 pA, 0.6 A/W, 3.4×10^{-15} W/Hz$^{1/2}$, and 8 GHz, respectively. All the parameters are comparable to those of similar devices made on InP substrate or other InGaAs products epitaxially grown on an InGaAlAs buffered GaAs substrate. The performances of the MM-PINPD on GaAs are analyzed by impulse injecting of 1.2-ps pulse-train, eye pattern at 10Gbps, and frequency response from VNA.

Keywords: Metamorphic, $In_{0.53}Ga_{0.47}As$, InGaP, GaAs, p-i-n Photodetector, receiver, OC-192.

1. INTRODUCTION

A long-wavelength optical transmission operating at 1.1 to 1.65 μm wavelength region has attracted considerable attention due to its low-loss and low dispersion optical characteristics. The semiconductor photodetectors, one of the key components, made on lattice-matched InP substrate, which offer advantages of low dark-current, high efficiency, and high speed operation, have been widely studied for optical fiber communication application. However, InP suffers from several drawbacks including higher fragility, less mature processing technologies, and smaller available wafer sizes compared to GaAs. Recently, different metamorphic (MM) epitaxial layers such as InGaAs [1], InAlAs [2], InAs [3], InGaAlAs [4], etc. have emerged as the buffered layers for growing InGaAs-based optoelectronic devices on GaAs substrates, such as high electron mobility transistor (HEMT), or heterojunction bipolar transistor (HBT), in optoelectronic integrated circuits (OEIC) for 40 Gbit/s and 80 Gbit/s applications have been presented [5-7]. Compositionally graded metamorphic buffer layers are extensively utilized to accommodate large lattice mismatch between a semiconductor substrate and epitaxial layers, which overcomes the limitation of band-gap engineering imposed by the substrate lattice parameters. Technically, the metamorphic epitaxy facilitates some advantages from greater strength, no need of InP substrate, ready availability of large diameter substrates, easier material handling, and the compatibility with the existing manufacturing infrastructure. These lead to a cost effective solution without sacrificing the device performance. Nevertheless, the rapid increase of data- or metro-communication has demanded huge capacity of optical communication systems. For such demand, the system of 10Gbps Ethernet (10GBE) actively investigated. For the key components to develop such a system, low-cost manufacture and high performance are strong required to advance the date of replacing one Gigabit Ethernet (GBE).

In previous work, we reported for the first time the performance of top-illuminated metamorphic p-i-n photodiodes (MM-PINPD) on GaAs substrates using linearly graded $In_xGa_{1-x}P$ buffer layer. The ultralow leakage of only 13 pA at a bias of -5 V can bring significant improvement in receiver sensitivity. The optical responsivities of 0.77 A/W and 0.6 A/W, and the NEP of 2.7×10^{-15} W/Hz$^{1/2}$ and 3.4×10^{-15} W/Hz$^{1/2}$, have been determined at 1310 nm and 1550 nm, respectively. In this work, to further analysis the high-frequency characteristic of the MM-PINPD, we propose the

Optoelectronic Materials and Devices for Optical Communications,
edited by Shinji Tsuji, Jens Buus, Yi Luo, Proc. of SPIE Vol. 6020,
602023, (2005) · 0277-786X/05/$15 · doi: 10.1117/12.636697

Downloaded From: http://proceedings.spiedigitallibrary.org/ on 04/26/2014 Terms of Use: http://spiedl.org/terms

fabrication of the MM-PINPD with coplanar pad on GaAs substrate for microwave probe and shorter length of wire bond. The impulse responses with injecting 1.2-ps pulse-train, generated by mode-locked semiconductor optical amplifier fiber laser (SOAFL), eye pattern at 10Gbps, the bit error rate (BER), the frequency response, and the sensitivity of MM-PINPD with a transimpedance amplifier (TIA) are reported.

2. EXPERIMENT SETUP

The MM-PIN heterostructure was grown on a 3-in (100)-oriented n-type GaAs substrate using gas source molecular beam epitaxy, as shown in Fig. 1(a). The two n-type contacts of 80 μm are in both sides of p-type contact of 80 μm with distance of 70 μm and this design is for connection with high frequency coplanar probe to improve performance of transmission, as shown in Fig. 2. A Si_3N_4 dielectric layer was deposited on the active region (with diameter of 60 μm) of the MM-PINPD device surface for passivation and antireflection. The MM-PINPD was connected with a 40-GHz probe (Picoprobe 40A-GSG-70-P) which uses a 50 ohm coaxial cable from the probe tips to K connecter. The center tip of this coplanar (Ground/Signal/Ground) probe was connected with the p-type contact on MM-PINPD and the two side tips were both connected with n-type contact. A bias-tee circuit was employed to combine negatively bias voltage and the responded signal of the MM-PINPD. The responsivity linearity and responsivity vs. wavelength ranged from 1310-nm to 1550-nm were determined using tunable lasers (Hewlett Packard, 8168F) and distributed feedback laser diodes (DFBLDs) in connection with an attenuator (Agilent, 8156a).

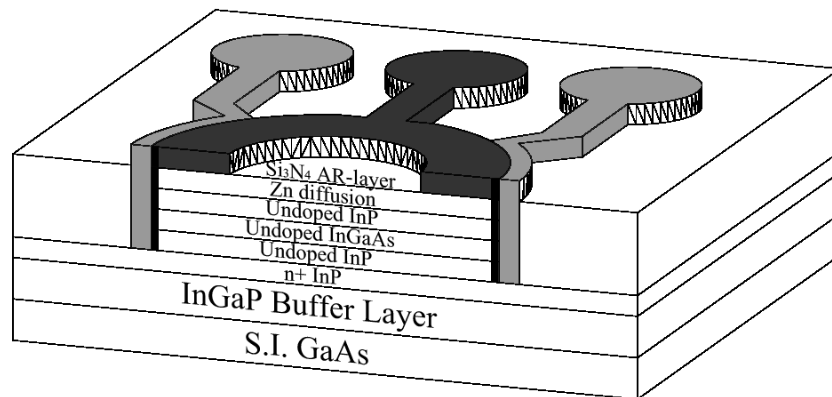

Fig. 1. The layer structure of a MM-PINPD on GaAs.

On the other hand, a nonlinearly soliton-compressed pulsewidth of 1.2 ps at repetition frequency for 1 GHz is used for impulse source which is generated by a backward dark-optical comb injection induced optically harmonic mode-locking of a semiconductor optical amplifier (SOA) based fiber laser (referred as SOAFL). We assembled the MM-PINPD by packaging the transimpedance into a TO46 housing. A signal lens was used to couple the light from a single mode fiber onto photodiode. The coupling loss for the non-optimized coupling was in the order of 4dB. To reduce parasitical inductances, parallel bond wires were used to connect the output of the photodiode to the lead of preamplifier. The temporal response of the MM-PINPD was monitored on a digital sampling oscilloscope (Agilent/HP 86100A+86116A, f_{3dB} > 63 GHz and t_{FWHM} = 7.5 ps). All measurements were conducted at room temperature.

.

Downloaded From: http://proceedings.spiedigitallibrary.org/ on 04/26/2014 Terms of Use: http://spiedl.org/terms

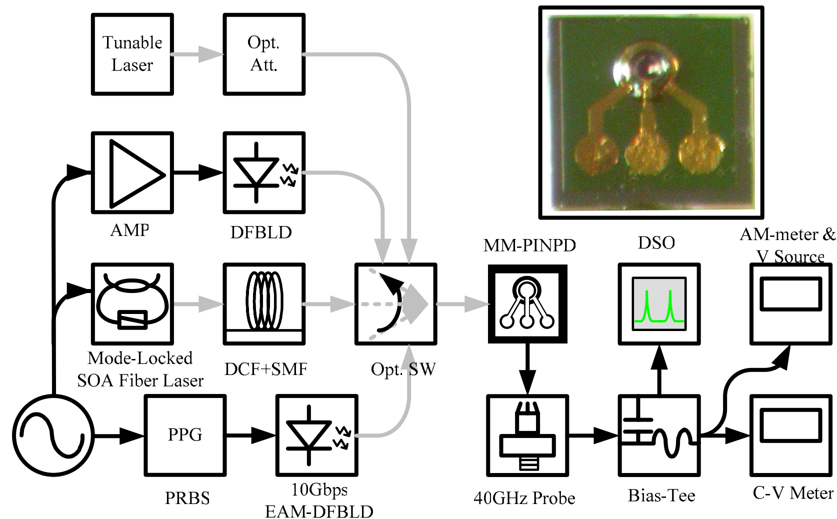

Fig. 2. The diagnostic setup for the SMA mounted InGaAs MM-PINPD on GaAs. Amp.: electrical amplifier, Atten.: optical attenuator, DFB-LD: distributed feedback laser diode, DSO: digital sampling oscilloscope.

3. RESULTS AND DISCUSSION

In general, a thick InGaP buffer layer can generate a high density of defects that results in high dark currents because of the unfiltered lattice-mismatch strain and the difference in thermal expansion coefficients between InGaP and the GaAs substrate. Therefore, the magnitude of dark currents could reflect the quality of InGaP metamorphic layer. As shown in Fig. 3(a), an InGaAs PINPD with a very low dark current density of 3.4×10^{-4} A/cm^2 at bias of 5 V and an optical responsivity of 0.55 A/W at 1550nm by using such a metamorphic buffer was reported. Such a low dark current reveals the better lattice grading property between the InGaP buffer and the GaAs substrate in this study. At a reverse bias of 5 V, The photocurrents measured at the illuminating power of 0 dBm is 0.6 mA, corresponding to an optical responsivity of 0.6 A/W. The photocurrent of MM-PINPD decreases from 0.6 mA to 0.6 nA as the illuminating power attenuates from 0 dBm to -60 dBm, while a linear relationship between the illuminating power and the corresponding photocurrent is found, as shown in Fig. 3(b). The responsivity of the MM-PINPD is extremely linear, which is even detectable at the illuminating power of below 100 pW due to its extremely low dark current. Moreover, the photocurrents and optical responsivities at 1310 nm and 1550 nm were also shown in Fig. 3(b) and 3(c). The power- and bias-dependent photocurrent of MM-PINPD illuminated at 1550-nm wavelength is shown in the Fig. 3(d). Under an illuminating power of 0 dBm, the optical responsivities at 1310 nm and 1550 nm are 0.77 and 0.6 A/W, respectively.

For evaluating the real response of the MM-PINPD, a delta function with full width at half maximum (FWHM) of 1.2 ps is generated by semiconductor optical amplifier fiber laser (SOAFL) [8]. The eighth-order soliton with pulsewidth of 1.2 ps is generated from a backward dark-optical-comb injection mode-locked SOAFL after linear dispersion compensation and nonlinear soliton compression. The dark-optical-comb with pulsewidth of 60 ps is performed by connecting a continuous-wave laser diode with an electrical-comb modulated Mach-Zehnder interferometer. After linear dispersion compensating in a 420m-long dispersion compensated fiber and nonlinearly soliton compressing in a 112m-long single-mode fiber under a high input power, which results in the pulsewidth, linewidth and the nearly transform-limited time-bandwidth product of 1.2 ps (de-convolution from an auto-correlator trace), 13.8 nm and 0.34, respectively.

Otherwise, by using a gain switched DFBLD with a pulse width of 42 ps and an average power of 0.1 mW at a repeating rate of 1 GHz, the switching responses of the MM-PINPD corresponding to the gain-switched pulse-train and the compressed pulse-train of mode-locked SOAFL, respectively, are also shown in the Fig. 4. Nevertheless, it is notable that MM-PINPD has excellence performance on rising time and falling time. The rising time of the MM-PINPD illuminated at gain-switched DFBLD and mode-locked SOAFL are 34.36 ps and 38.55 ps, respectively. The switching time is less than 80 ps. The measured frequency characteristics of the MM-PINPD by using Lightwave Component Analyzer (Agilent/HP 8703A, 0.13 ~20 GHz) at 1.55um wavelength and the MM-PINPD's -3dB and -6dB bandwidth of larger than 8GHz and 12GHz was shown in the inset of Fig. 4.

Downloaded From: http://proceedings.spiedigitallibrary.org/ on 04/26/2014 Terms of Use: http://spiedl.org/terms

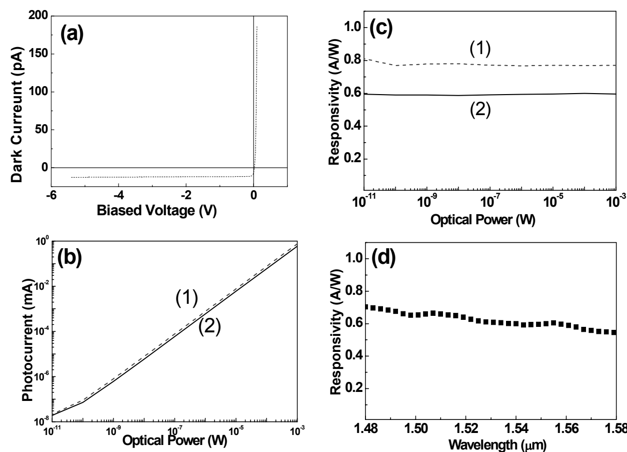

Fig. 3. (a): Dark current versus biased voltage from 0.1 V to -5 V for MM-PINPD, showing a 13 pA leakage current at -5V. (b): The responsivities of the MM-PINPD at different wavelengths and powers at (1) 1310 nm and (2) 1550 nm. (c) The optical photocurrents of the MM-PINPD as a function of optical power (d): wavelength dependence around 1550nm.

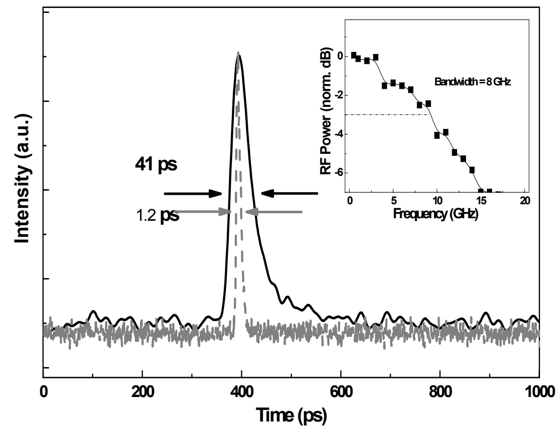

Fig. 4. The optoelectric power transfer characteristics of MM-PINPD at 1550 nm. The inset shows the temporal traces of the MM-PINPD under the illumination of a 1.2-ps mode-locked SOAFL at repetition frequency of 1 GHz.

A further test of the broadband conversion capability was done with in an electronic time division multiplexing (ETDM) experiment using a 10 Gbit/s optical data stream (NRZ 2^7-1 pattern length PRBS, optical input power -6dBm). The measured eye pattern at the MM-PINPD output was shown in the inset of Fig. 5 which was connected with a GSG probe using a 50 ohm coaxial cable. A 1550-nm semiconductor laser with $LiNbO_3$ modulator was used as the optical source. It is seen that well-opened eye diagram are obtained for dynamic range. The noise on the eye pattern is mainly attributed to the absence of the transimpedance amplifier (TIA) and the amplitude (10mV) is near the NEP of our sampling scope. On the other hand, the bit error rate measurements of the MM-PINPD with transimpedance amplifier were performed. The transmitter was the same as was used for the eye pattern measurements. As can be seen from Fig. 5, sensitivities of -20.3, -19.5 and -17.6 dBm were obtained for date rate of 8, 10, and 12 Gbit/s, respectively, at a bit error rate of 10^{-9}. The leakage current density of 3.6×10^{-7} A/cm^2 for the InGaP-buffered MM-PINPD on GaAs is ultra low, and it is almost two to three orders of magnitude smaller then the other InGaAs PINPD using such a metamorphic buffer[9]. Such a low dark current reveals the better lattice grading property between the InGaP buffer and the GaAs substrate in this study. The leakage current of photodetector influence the noise equivalent power of the receiver module, and exceeding high leakage is one factor of deciding sensitivity. Reducing the device leakage current can bring significant improvement in receiver sensitivity. Such the responsivity of 0.6A/W at 1.55um is not an amazed result even though, but the ultralow leakage and matched bandwidth are important advantages for using in 10-Gbit/s fiber optics communication.

Downloaded From: http://proceedings.spiedigitallibrary.org/ on 04/26/2014 Terms of Use: http://spiedl.org/terms

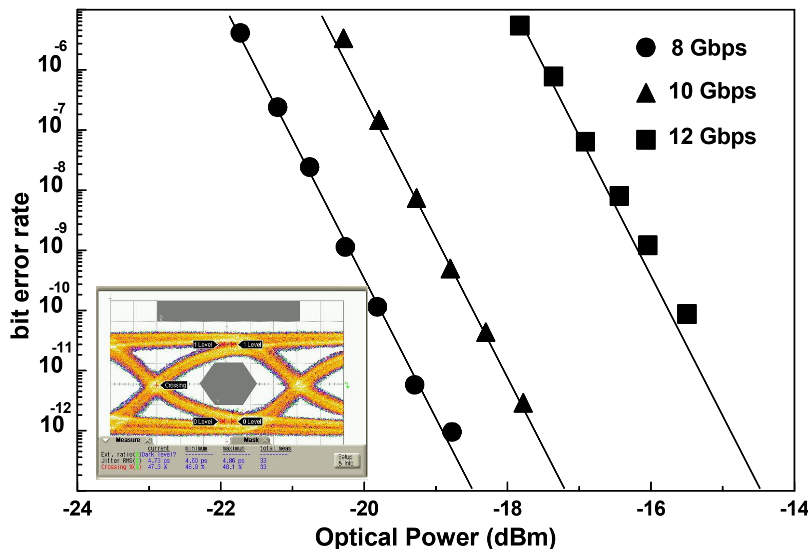

Fig. 5. The BER analysis of InGaAs PINPD-TIA receiver at different data rates. The inset shows the measured 10Gbit/s eye pattern of the MM-PINPD with TIA.

4. CONCLUSION

In conclusion, low-leakage $In_{0.53}Ga_{0.47}As$ p-i-n photodetector fabricated on GaAs substrate with linearly graded metamorphic $In_xGa_{1-x}P$ buffer layer has been demonstrated. At a bias of -5 V, the MM-PINPD exhibits a dark current of only 13 pA. The optical responsivities of 0.77 A/W and 0.6 A/W, and the NEP of 2.7×10^{-15} W/Hz$^{1/2}$ and 3.4×10^{-15} W/Hz$^{1/2}$, have been determined at 1310 nm and 1550 nm, respectively. The DC, radio frequency, and communication performance of the low-leakage $In_{0.53}Ga_{0.47}As$ p-i-n photodetector fabricated on GaAs substrate with linearly graded metamorphic $In_xGa_{1-x}P$ buffer layer are characterized. All the parameters are comparable to those of similar devices made on InP substrate or other InGaAs products epitaxially grown on an InGaAlAs buffered GaAs substrate. The operational bandwidth can be up to 8 GHz without reducing the diameter of aperture and managing the reflected signal by impedance matching. The sensitivities of -20.3, -19.5 and -17.6 dBm with standard TO-46 package were obtained for date rate of 8, 10, and 12 Gbit/s, respectively. The demonstrated metamorphic epitaxy is particularly suitable for mass-production of such devices on GaAs substrates and is also suitable for commercial TO-can based OC-192 PIN-TIA receiver.

ACKNOWLEDGEMENT

This work was supported in part by the National Science Council (NSC) of the Republic of China under grant NSC 93-2215-E-009-007 and NSC 94-2215-E-009-040.

REFERENCES

1. L. Pavesi, L. Dal Negro, C. Mazzoleni, G. Franzo, and F. Priolo, “Optical gain in silicon nanocrystals,” *Nature (London)*, vol. 408, pp. 440-444, 2000.
2. Q. Ye, R. Tsu, and E. H. Nicollian, “Resonant tunneling via microcrystalline-silicon quantum confinement,” Phys. Rev. B, vol. 44, pp. 1806-1811, 1991.
3. A. Pèrez-Rodrìguez, O. González-Varona, B. Garrido, P. Pellegrino, J. R. Morante, C. Bonafos, M. Carrada, and A. Claverie, “White luminescence from Si^+ and C^+ ion-implanted SiO_2 films,” J. Appl. Phys., vol. 94, pp. 254-262, 2003.
4. D. Pacifici, E. C. Moreira, G. Franzo, V. Martorino, and F. Priolo, “Defect production and annealing in ion-irradiated Si nanocrystals,” Phys. Rev. B, vol. 65, pp. 1441091-1-13, 2002.
5. K. Toshikiyoa, M. Fujiib, and S. Hayashia, ”Enhanced optical properties of Si nanocrystals in planar microcavity,” Phys. E, vol. 17, pp. 451-452, 2003.
6. M. C. Rossi, S. Salvatori, F. Galluzzi, and G. Conte, “Laser-induced nanocrystalline silicon formation in a-SiO matrices,“ Mater. Sci. Eng. B, vol. 69-70, pp. 299-302, 2000.

Downloaded From: http://proceedings.spiedigitallibrary.org/ on 04/26/2014 Terms of Use: http://spiedl.org/terms

7. A. Janotta, Y. Dikce, M. Schmidt, C. Eisele, M. Stutzmann, M. Luysberg, and L. Houben, “Light-induced modification of a-SiOx II: Laser crystallization,” J. Appl. Phys., vol. 95, pp. 4060-4068, 2004.
8. B. Gallas, C.-C. Kao, S. Fisson, G. Vuye, J. Rivory, Y. Bernard, and C. Belouet, “Laser annealing of SiOx thin films,” Appl. Surf. Sci., vol. 185, pp. 317-320, 2002.
9. E. D. Palik, Handbook of Optical Constants of Solids, p. 762, Academic Press, Washington, 1985.
10. T. R. Shiu, C. P. Grigoropoulos, D. G. Cahill, and R. Greif, “Mechanism of bump formation on glass substrates during laser texturing,” J. Appl. Phys., vol. 86, pp. 1311-1316, 1999.
11. J. Zhao, J. Sullivan, J. Zayac, and T. D. Bennett, “Structural modification of silica glass by laser scanning,” J. Appl. Phys., vol. 95, pp. 5475-5482, 2004.
12. A. R. Forouhi and I. Bloomer, “Optical dispersion relations for amorphous semiconductors and amorphous dielectrics,” Phys. Rev. B, vol. 34, pp. 7018-7026, 1986.
13. A. R. Forouhi and I. Bloomer, “Optical properties of crystalline semiconductors and dielectrics,” Phys. Rev. B, vol. 38, pp. 1865-1874, 1988.
14. A. R. Forouhi and I. Bloomer, U.S. Patent No. 4,905,170.
15. F. Iacona, G. Franzo, E. C. Moreira, D. Pacifici, A. Irrera, and F. Priolo, “Luminescence properties of Si nanocrystals embedded in optical microcavities,” Mater. Sci. Eng. C, vol. 19, pp. 377-381, 2002.
16. G. V. Prakash, M. Cazzanelli, Z. Gaburro, L. Pavesi, F. Iacona, G. Franzo, and F. Prilolo, “Linear and nonlinear optical properties of plasma-enhanced chemical-vapor deposition grown silicon nanocrystals,” J. Modern Opt., vol. 49, pp. 719-730, 2002.
17. L. Khriachtchev, M. Rasanen, S. Novikov, and L. Pavesi, “Systematic correlation between Raman spectra, photoluminescence intensity, and absorption coefficient of silica layers containing Si nanocrystals,“ Appl. Phys. Lett., vol. 85, pp. 1511-1513, 2004.
18. A. E. Naciri, M. Mansour, L. Johann, J. J. Grob, and C. Eckert, “Correlation between silicon nanocrystalline size effect and spectroscopic ellipsometry responses,” Thin Solid Films, vol. 455-456, pp. 486-490, 2004.
19. G.-R. Lin, C. J. Lin, and C. K. Lin, “Defect-enhanced photoconductive response of silicon-implanted borosilicate glass,” Appl. Phys. Lett., vol. 85, pp. 935-937, 2004.
20. H. Nishikawa, R. Nakamura, and J. H. Stathis, “Oxygen-deficient centers and excess Si in buried oxide using photoluminescence spectroscopy,” Phys. Rev. B, vol. 60, pp. 15910-15918, 1999.
21. J. C. Cheang-Wong, A. Oliver, J. Roiz, and J. M. Hernanaez, “Optical properties of Ir_2^+-implanted silica glass,” Nucl. Instrum. Methods Phys. Res. B, vol. 175, pp. 490-494, 2001.

Downloaded From: http://proceedings.spiedigitallibrary.org/ on 04/26/2014 Terms of Use: http://spiedl.org/terms